FUNCTIONAL CHARACTERIZATION OF RNA BINDING PROTEIN CAPRIN2 IN MOUSE EYE DEVELOPMENT

by

Nathaniel Borders

A thesis submitted to the Faculty of the University of Delaware in partial fulfillment of the requirements for the degree of Honors Degree in Biological Sciences with Distinction

Spring 2017

FUNCTIONAL CHARACTERIZATION

OF RNA BINDING PROTEIN CAPRIN2

IN MOUSE EYE DEVELOPMENT

by

Nathaniel Borders

Approved: _____

Salil Lachke, PhD
Professor in charge of thesis on behalf of the Advisory Committee

Approved: _____

Melinda Duncan, PhD
Committee member from the Department of Biological Sciences

Approved: _____

Tania Roth, PhD
Committee member from the Board of Senior Thesis Readers

Approved: _____

Michael Arnold, Ph.D.
Directory, University Honors Program

ACKNOWLEDGMENTS

I would like to thank Dr. Lachke for allowing me to conduct research in his lab and mentoring me in the process of becoming a better scientific thinker. I have learned an extremely varied set of scientific skills and techniques in lab that I will be able to apply to my future as a scientist. In addition, the importance of precise and understandable language that was highly stressed will serve me very well. Thank you Lachke Lab members, both past and present, for being warm, welcoming, and helpful throughout my career here. You made my lab day-to-day lab experience a lot of fun. Thank you Soma Dash for being such an amazing mentor. Your infinite patience gave me the space to learn not only specific techniques, but also how to be a more organized and effective person. I would also like to thank my committee members Dr. M. Duncan and Dr. Roth for their guidance and analysis on this project. Finally, a big thanks to my family, friends, and girlfriend for their support throughout this process.

TABLE OF CONTENTS

LIST OF FIGURES

ABSTRACT

The *iSyTE* bioinformatics tool developed by the Lachke laboratory previously identified that a novel RNA binding protein (RBP) and RNA granule component, Caprin2, is enriched in the mouse lens at the early embryonic (E) day 10.5 and later stages. It was demonstrated that Caprin2 mRNA and protein were localized to lens fiber cells, supporting the hypothesis that it has potential function in lens development. It was also demonstrated that a lens-specific conditional mouse knockout of *Caprin2* (*Caprin2*$^{cKO/cKO}$) resulted in nuclear fiber cell compaction and a persistent lenti-corneal stalk. However, the lenti-corneal stalk phenotype was only observed at 8% penetrance in *Caprin2*$^{cKO/cKO}$ mouse eyes. We hypothesized that one of the reasons for the low penetrance of this ocular defect may result from residual Caprin2 protein present at E12.5 in the mutant mice. Therefore, *Caprin2* germline (*Caprin2*$^{-/-}$) deletion knockout mouse mutants that would lack Caprin2 protein earlier in embryogenesis were generated to test this hypothesis. Phenotypic characterization involving histology and scanning electron microscopy did not reveal any obvious ocular defects in *Caprin2*$^{-/-}$ mice. Further analyses revealed that Caprin1, a paralogous RNA binding protein, is upregulated in the *Caprin2*$^{-/-}$ lens. Interestingly, while Caprin1 protein levels were elevated, its mRNA was not found to be significantly different in *Caprin2*$^{-/-}$ lenses at E14.5, suggesting a potential post-transcriptional mechanism as the basis of the Caprin1 up-regulation in the mutant lens. These findings suggest that removal of

Caprin2 earlier in embryogenesis causes the up-regulation of Caprin1 that may result in redundancy and "rescue" of the ocular defects observed in *Caprin2*$^{cKO/cKO}$ mouse eyes. Therefore, *Caprin1* and *Caprin2* double knockout mouse mutants may need to be generated to test this hypothesis in the future.

Chapter 1

INTRODUCTION

1.1 The Mammalian Optic Lens

The mammalian optic lens is a transparent tissue located behind the cornea in the anterior portion of the eye (Figure 1.1). When light enters the cornea, it is gathered and refracted through the pupil onto the surface of the lens. The refractive properties of the lens and cornea allow them to focus the light onto the retina in the posterior portion of the eye, where specialized photoreceptor cells respond to photons and transmit this information via other cells to the optic nerve. The optic nerve then carries the signal to the brain where it is interpreted as brightness, contrast, and color (Graw, 2003).

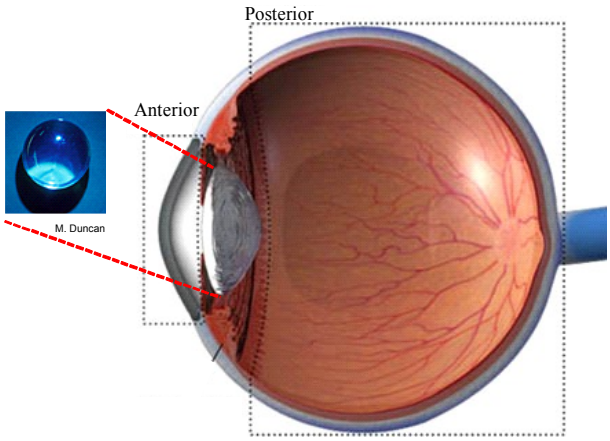

Figure 1.1: The mammalian optic lens is located in the anterior part of the eye and is posterior to the cornea and anterior to the retina and aqueous humor (Duncan, 2012).

The optic lens provides the advantage of high-resolution vision and in humans, also allows "accommodation" which is the ability to focus on objects at varying distances or depths. To achieve such adaptability the lens has to coordinately function with other components of the eye. The unique physical properties of the lens, namely its flexibility and transparency, are highly regulated and maintained and when either is disrupted, loss of vision occurs (Donaldson, 2001). Lens opacity, which is also known as cataract, affects the vision of half of Americans over the age of 75 (https://nei.nih.gov/eyedata/cataract).

Eye development is a highly controlled process, where even small alterations in its regulation or mutations/deletions of key genes result in defects. Eye development defects include congenital cataracts, microphthalmia (abnormally small eye), anophthalmia (no eye), and aniridia (Graw, 2003).

Lens development in mice begins at embryonic day (E) 9.5, when the optic vesicle interacts with the overlying surface ectoderm and results in its "thickening" into the lens placode (Figure 1.2). Further into development, the invagination of the lens placode forms the lens pit at E10.0 and by E10.5 the lens pit forms the lens vesicle (Cvekl, 2014). As the lens vesicle undergoes a process called apical constriction, the ectoderm that will contribute to the future cornea separates from the developing lens vesicle at E11.0. Epithelial cells at the posterior region of the lens vesicle exit the cell cycle, and elongate to fill the lumen of the lens vesicle. These are termed as primary fiber cells.

At later development stages, epithelial cells that are near the equator of the lens differentiate into secondary fiber cells – a process that continues throughout the life of the organism. These events involve the continued proliferation of the cuboidal anterior

epithelial cells at the zone of proliferation located just anterior to the equator of the lens. The lens is subjected to a posterior (high) to anterior (low) fibroblast growth factor (Fgf) gradient that induces epithelial cells near the equator to exit the cell cycle within what is called as transition zone and differentiate into elongated secondary fiber cells. Fiber cell differentiation involves organelle degradation (Cvekl, 2014), which is essential for lens transparency (Figure 1.2).

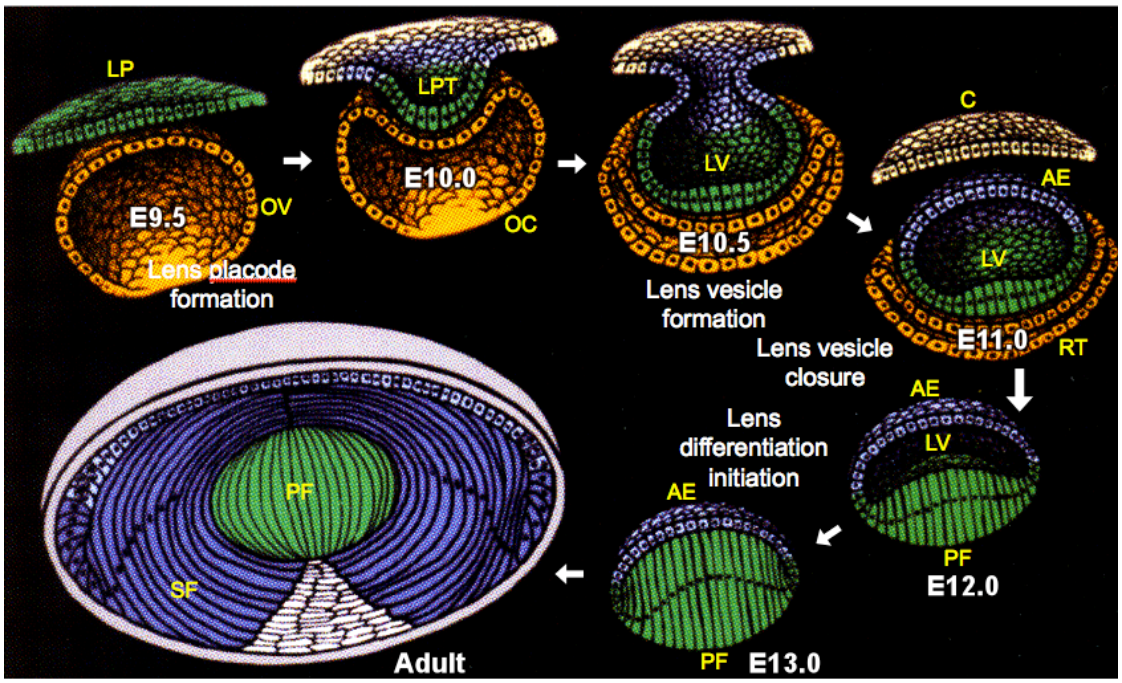

Figure 1.2: Embryonic development of the mouse lens. Beginning at E9.5 the surface ectoderm thickens to form the lens placode. The lens placode invaginates to form the lens pit at E10.0. By E10.5 the lens pit further invaginates to form the lens vesicle. The corneal ectoderm pinches off from the developing lens vesicle at E11.0. The posterior epithelial cells of the lens vesicle elongate to fill the lumen of the lens vesicle. This process completes at E13.0 and secondary fiber cell differentiation begins, a process that will continue throughout the life of the organism (Kuszak and Brown, 1994).

Removal of organelles from the lens cells implicated in vision is necessary because the function of the lens depends on its ability to maximally refract light and the two inhibitions to this are light absorption and scattering. Light scattering occurs when the properties of the lens are altered, causing the normally tight focus of the lens to spread. For example, if the properties of the cortical lens fiber cells were to change, light would refract differently through that part of the lens and may not be properly projected on the retina, causing suboptimal vision.

In the mammalian lens, the refractive index of cytoplasm is close to water while the refractive index for organelles is much higher. Light that happens to hit an organelle would be forced to deviate from its original trajectory through the cytoplasm. Thus, organelle degradation serves to allow the light to refract at a constant rate and avoid scattering while moving through the lens (Bassnett, 2009).

1.2 Prediction of Eye Pathology Associated Genes

The traditional methods of eye gene discovery have proven to be challenging and time consuming. For example, roughly only 44 gene loci for congenital cataracts have been found to date (Shiels, 2016). A majority of these were identified through the lengthy process of gene mapping, linkage analysis, and sequence analysis of the genomic regions. With the advent of bioinformatics, we have the opportunity to analyze genomes and transcriptomes to prioritize key genes in specific tissues and their pathologies (Lachke, 2012).

The computational tool *iSyTE* (integrated Systems Tool for Eye gene discovery http://bioinformatics.udel.edu/Research/iSyTE), was developed as a resource tool that compares expression data from mouse embryonic lens to rank genes that may be implicated in the development of this tissue and its associated defects (Lachke, 2012).

iSyTE prioritizes genes based on their higher expression in the lens compared to their expression in whole embryonic body tissue (WB). This method of "WB *in silico* subtraction" has led *iSyTE* to identify a number of genes related to lens defects, which include: *Tdrd7, Pvrl3, Sep15, MafG, and MafK* (Agrawal, 2015; Kasaikina, 2011; Lachke, 2012; Lachke, 2011).

iSyTE has led to the identification of several RNA binding proteins (RBPs) that function in the lens. These proteins, such as Tdrd7, function in distinct types of post-transcriptional gene expression control. These include splicing and polyadenylation as well as mRNA stabilization and translation (Dash, 2016). Recently, the Lachke laboratory identified another such RBP Caprin2 that is highly expressed and enriched in the lens from E10.5, suggesting that this protein may potentially function in lens development or homeostasis.

1.3 Caprin2 and its Association with Peters Anomaly and Lens Compaction Defects

The RBP and RNA granule (RG) component Caprin2 (Cytoplasmic activation/proliferation associated protein 2) is a highly conserved molecule in metazoa with orthologs in *Drosophila*, chicken, mouse, and humans. Caprin2 belongs to the C1q and tumor necrosis factor super-family of proteins (Lorén, 2009). Caprin2 also contains coiled coil and RGG domains that potentially bind to RNA (Dash, 2015; Shiina and Tokunaga, 2010) (Figure 1.5).

Through *iSyTE*, *Caprin2* was found to exhibit highly enriched expression in the mouse lens compared to WB starting at E10.5. Caprin2 mRNA and protein are localized to the anterior rim of the lens pit at E10.5 and in the fiber cells of the lens

starting at E12.5, indicating that it may have a potential function in lens development (Figure 1.4).

Mice with lens-specific targeted knockout of *Caprin2* (*Caprin2*$^{cKO/cKO}$) (Figure 1.4) exhibit two defects, namely, compaction of the central region of fiber cells and an abnormal lenti-corneal stalk (Dash, 2015). Compaction of the central fiber cell region in adult lenses was detected by scanning electron microscopy (SEM) in all *Caprin2*$^{cKO/cKO}$ animals tested. In 8% of the *Caprin2*$^{cKO/cKO}$ mouse eyes, a feature of Peters anomaly characterized by the presence of a persistent lenti-corneal stalk was observed (Figure 1.6).

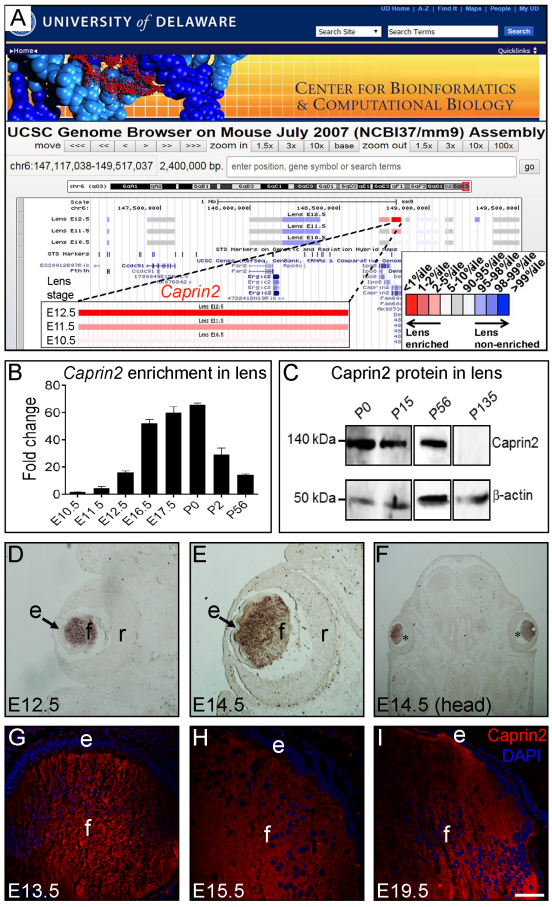

Figure 1.3: Caprin2 expression in the developing mouse lens. **A:** *iSyTE* identifies Caprin2 as being in the top 1% of lens enriched genes at embryonic stage (E) E12.5. **B:** Public mouse lens microarray data sets were analyzed to compare Caprin2 expression in the lens to the whole embryo body (Affymetrix). Caprin2 was enriched in the lens at all stages tested. **C:** Western blotting demonstrates that Caprin2 is highly expressed in early postnatal stages, peaking at P0, and decreasing to undetectable levels by P135. **D,E:** In situ hybridization (ISH) demonstrates high levels of expression of Caprin2 transcripts in the lens fiber cells (f), and no expression in the epithelium (e) or retina (r). **F:** A low magnification image of an E14.5 mouse head section shows specific Caprin2 expression in the lens fiber cells. **G–I:** Immunostaining of mouse head tissue at E13.5, E15.5, and E19.5 demonstrates specificity of Caprin2 protein to the lens fiber cells and not epithelium. (Dash, 2015).

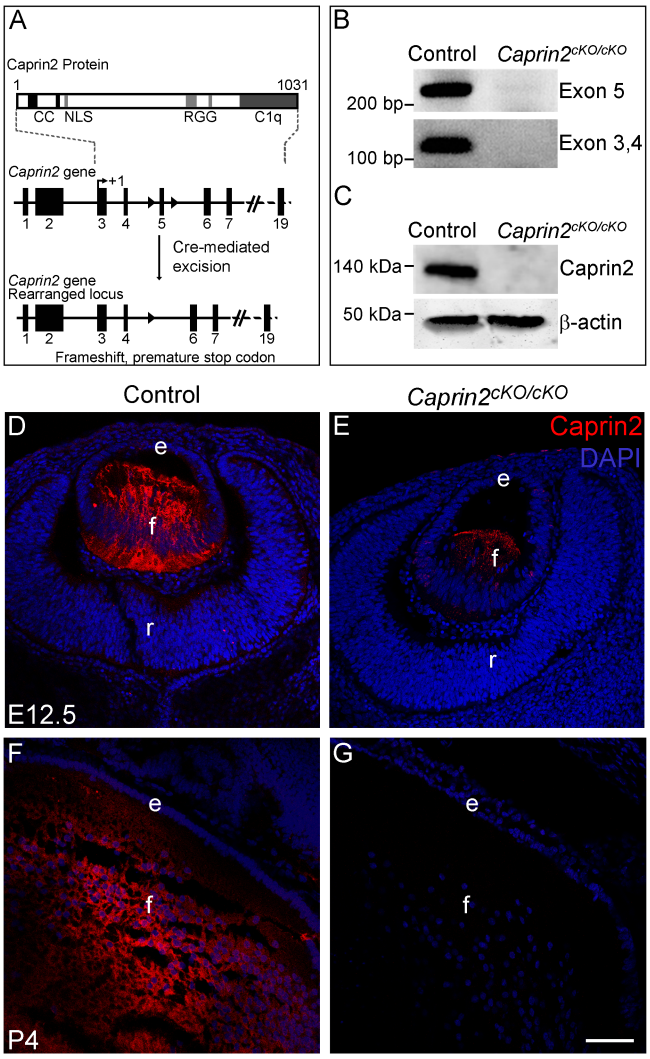

Figure 1.4: Generation of *Caprin2* lens-specific conditional knockout mouse mutants. **A:** The *Caprin2* gene locus and Caprin2 protein structure. LoxP sites denoted by closed arrowheads flank exon 5 of the *Caprin2* knockout allele. Cre recombinase expression leads to excision of Exon 5 of *Caprin2*. This causes a frame shift when exon 4 and 6 are abnormally joined, which is expected to introduce a premature stop codon. **B:** *Caprin2* mRNA in *Caprin2*$^{cKO/cKO}$ and control mice is examined by reverse transcriptase polymerase chain reaction. **C:** Western blotting demonstrates the absence of Caprin2 protein in mutant mice at P56. **D,E:** Immunostaining finds residual Caprin2 protein in *Caprin2*$^{cKO/cKO}$ mice at E12.5. **F,G:** By P4 there is no detectable expression of Caprin2 protein in the mutant lens.

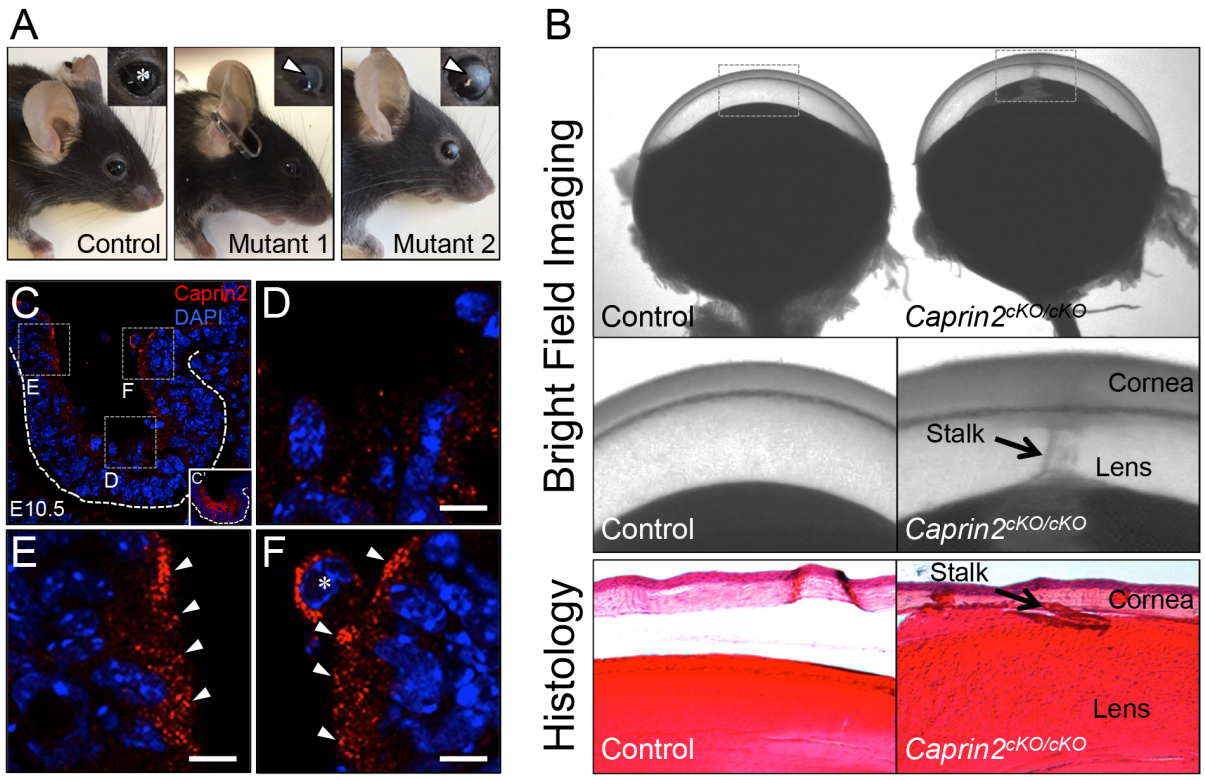

Figure 1.5: *Caprin2*$^{cKO/cKO}$ mouse mutants exhibit eye defects. **A:** Eye images (inset, high magnification) from control and representative mild (Mutant 1) and severe (Mutant 2) cases of lenti-corneal defect. White arrowheads indicate corneal opacity and asterisk denotes reflection of light. **B:** Dark field imaging and histology show that *Caprin2*$^{cKO/cKO}$ mutants have a lenti-corneal stalk. This was observed in about 8% of the eyes analyzed. **C:** Immunostaining shows that Caprin2 protein is localized in cells at the anterior rim of the lens pit (marked by dotted line) at stage E10.5. Broken line boxes in C indicate the regions shown in D, E, and F at high magnification. **C':** Jag1 immunostaining allows better visualization of E10.5 lens pit structure. **D:** Caprin2 protein expression is reduced in the posterior part of the pit. **E,F:** In the anterior rim region of the lens pit, Caprin2 protein exhibits a granular pattern (white arrowheads).

1.4 Lens Compaction Defect and Features of Peters Anomaly in *Caprin2*$^{cKO/cKO}$ mice

After primary fiber cells elongate, the lens undergoes secondary fiber cell differentiation. Throughout the life of the organism, secondary fiber cells continue to be added, surrounding the nuclear core of primary fiber cells. Nuclear compaction occurs with aging and is associated with age-related cataracts and diminished lens accommodation ability (Bassnett, 2016).

Clinical observation reveals strong evidence for the presence of lens compaction in humans. Physical trauma to the eye can result in an area of the lens becoming opaque. As normal transparent secondary fiber cell growth occurs, this opaque layer is buried deeper and deeper in the lens. In an analogous example, certain forms of congenital cataract only affect the nuclear or the proximal nuclear region. Thus, size and shape of the opaque nuclear region are easily visualized over the lifetime of the subject. In both cases, the distance between the opacifications and the lens surface continually increases (Bassnett, 2016). However, the overall size and weight of the lens increases at a much-decreased rate. Instead, the dry weight (organelles, cell membranes, etc.) increases over time, while the nuclear fiber cells dehydrate and shrink. This principle allows for continuous addition of secondary fiber cells without the lens becoming too large or heavy (Bassnett, 2016).

The mammalian lens relies on a differential of refractive index between the nuclear (n = 1.402) and cortical (n = 1.381) lens to bend and therefore focus light. The refractive index is a measure of how much the light is bent and interfered with. In this case, light in a vacuum travels 1.381 times faster than through the cortical fiber cells. This allows light to take a longer path through the outer fiber cells and take less time traveling through the inner fiber cells and then converge at the same time at the focal

point on the retina to produce a coherent image. These refractive gradients are delicately maintained through control of protein gradient (Bassnett, 2016).

If nuclear compaction occurs too quickly, due to abnormal genetic regulation, the lens shows signs of age related disease. Pathological nuclear fiber cell compaction in humans is associated with cataract formation and loss of accommodative capability (Al-Ghoul, 2001).

Peters anomaly is a developmental defect caused due to the persistence of a lenti-corneal stalk, corneal opacity, and defects in the posterior cornea (Bhandari, 2011). These defects hinder the ability of the cornea to transmit light and therefore lead to a loss in visual acuity (Graw 2003). In addition, Peters anomaly has been linked to glaucoma caused by malformation of the trabecular meshwork, a tissue responsible for draining the aqueous humor behind the cornea (Weh, 2014; Sampaolesi, 2009). It should be noted that in cases where functional compromise or deficiency of genes such as *PAX6*, *PITX2*, and *FOXE3* that results in Peters anomaly, this specific defect is observed at incomplete penetrance (Hanson, 1994; Reis 2012; Ormestad 2002).

Developmentally, abnormal regulation of the process of apical constriction of the lens vesicle and cornea causes Peters anomaly. One of the mechanisms behind this event involves p120-catenin mediation of Shroom3 binding to adherens junctions. In wildtype lens tissue, Shroom3 associates with adherens junctions, leading to the contraction of the apical side of the epithelial cell. This causes cuboidal cells to become a wedged shape, leading to invagination of the lens placode into the lens pit at E10.5. In addition, the cells at the anterior rim of the lens pit must come together and form adherens junctions with each other. This leads to the closure of lens vesicle and

separation of the lens and cornea by E11.0. Loss of Shroom3 function results in a loss of the hinge points that allow for proper separation of the lens and cornea, which produces a Peters anomaly-like phenotype (Lang, 2014).

1.5 Further Investigation into the Caprin2 Mutant Lens Phenotype

Caprin2$^{cKO/cKO}$ lenses expressed both nuclear compaction and features of Peters anomaly allowing *Dash et al.* to conclude that Caprin2 has important developmental function in the lens. However, due to the low penetrance of the lenti-corneal stalk phenotype, further investigation into the function of Caprin2 was required.

A possible reason for the low penetrant phenotype could be in the mouse knockouts generated. In *Dash et al.,* mice carrying *Caprin2* conditional null alleles were crossed with *Pax6GFPCre* mice, where beginning at E8.75 Cre recombinase expression is driven by the *Pax6* ectodermal enhancer in the lens fated cells. It was observed that at E12.5 *Caprin2*$^{cKO/cKO}$ mutant mouse lenses expressed residual Caprin2 protein (Figure 1.6 E). As key events relating to Peters anomaly occur between E10.0 and E11.0, the deletion of *Caprin2* occurred by a sufficiently late time point that it may have influenced the development of the lens and specifically resulted in a low penetrant phenotype. Therefore my hypothesis is that residual Caprin2 protein results in a low penetrance Peters anomaly phenotype.

Another possible hypothesis for the low penetrant Peters anomaly phenotype is the expression of *Caprin2* paralog *Caprin1*. The reason for this is that in the case of low penetrance of a phenotype due to the knockout of a gene, it is common that a redundant protein compensates for the deficient protein. Caprin1 is an RNA granule protein, contains RGG boxes, and basic helix domains like Caprin2. However, *iSyTE*

has shown that it is not lens enriched, but that it is lens expressed and that there is no significant difference in Caprin1 protein or RNA expression in *Caprin2*$^{cKO/cKO}$ lenses. Caprin1 protein expression is detected in cells at the rim of the lens pit at E10.5, similar to Caprin2, in both wild type and *Caprin2*$^{cKO/cKO}$ mice. Therefore, I posit that *Caprin1* expression may also compensate for the absence of Caprin2 in *Caprin2*$^{cKO/cKO}$ lenses. In this Senior thesis, I tested these hypotheses by generating *Caprin2*$^{-/-}$ mice and characterizing their ocular tissue.

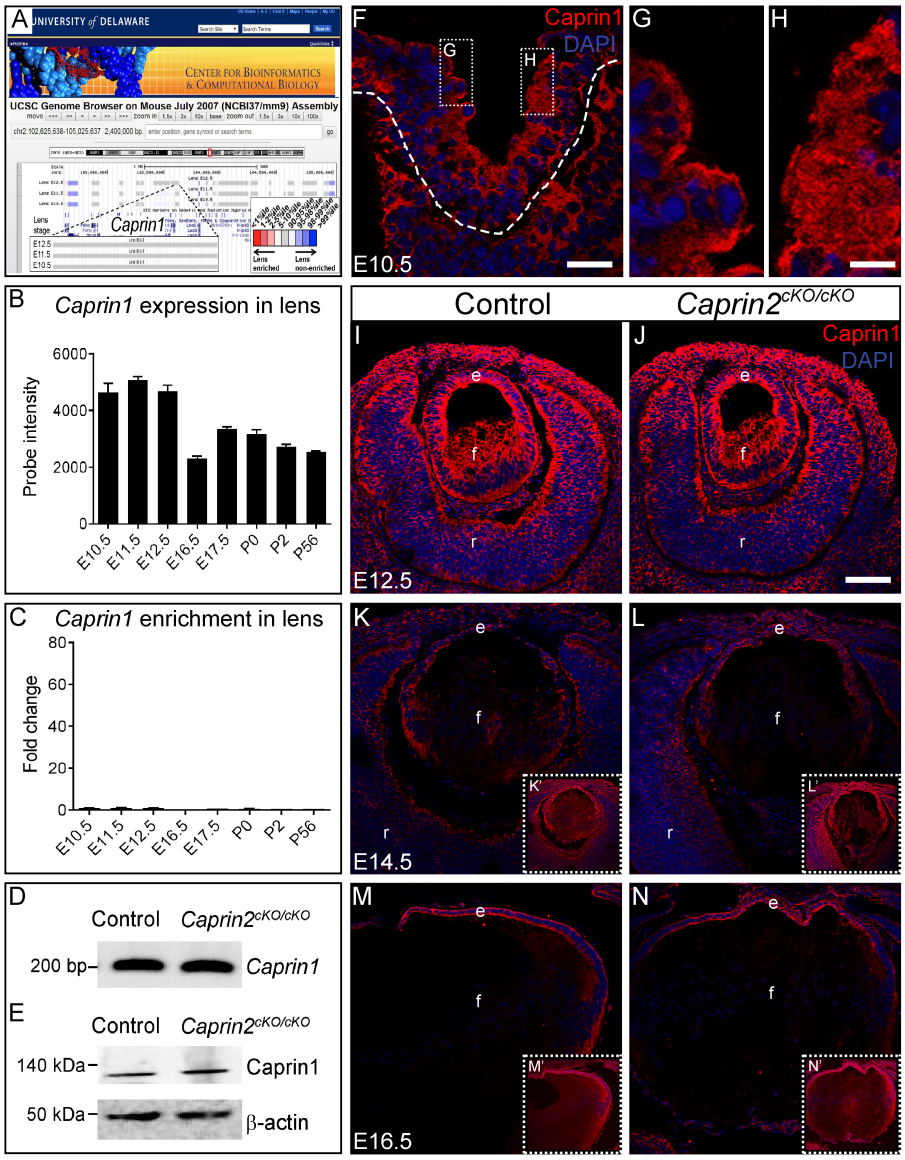

Figure 1.6: Caprin1 is highly expressed, but not enriched in the developing mouse lens. **A,C:** *iSyTE* reveals that while it is expressed in the lens, *Caprin1* is not signifincanly lens-enriched. **B:** Microarray analysis shows high levels of *Caprin1* expression in the developing and juvenile mouse. **D:** There is no difference in *Caprin1* mRNA expression between control and *Caprin2*$^{cKO/cKO}$ mice as examined by RT-PCR analysis. **F-H:** Immunostaining of Caprin1 protein at E10.5 reveals high expression levels (F) and localization to the anterior rim of the lens pit cells (G, H). **I-N:** Immunostaining of Caprin1 protein suggests no alteration in control and mutant lenses.

Chapter 2

METHODS

2.1 Animals

Mice used in this investigation were housed in University of Delaware animal facility. The University of Delaware Institutional Animal Care and Use Committee (IACUC) approved all experimental protocols that include animals. All animal experiments were performed under the guidance of the Association of Research in Vision and Ophthalmology (ARVO) statement for use of animals in ophthalmic and vision research. Mice with the *Caprin2*$^{tm2a(EUCOMM)Wtsi}$ allele (referred to hereafter as *Caprin2*$^{flox/flox}$) were generated by the Welcome Trust Sanger Institute and obtained from the European Mouse Mutant Archive (EMMA), (EMMA ID, EM:05381). Tg(CMV-cre)1Cgn mice expressing germline Cre recombinase driven by the CMV promoter in early embryonic development were also used. The construct used and protocol for the deletion strategy is available at www.infrafrontier.eu and www.informatics.jax.org/alleleMGI:4434168. A minimum of 2 to 3 biological replicates was used; however, in the case of E11.5 *Caprin2*$^{-/-}$ mouse lenses stained for Caprin1 only one mutant lenses was analyzed.

2.2 Generation of *Caprin2* Germline Deletion Mouse Mutants

To delete *Caprin2* constitutively, *Caprin2*$^{flox/flox}$ mice were crossed with *Cre*$^{+/-}$ mice. One in four progeny of this cross has the genotype *Caprin2*$^{+/flox}$;*Cre*$^{+/-}$, where one *Caprin2* allele is deleted in the whole body. Further crosses resulted in *Caprin2*$^{flox/flox}$;*Cre*$^{+/-}$ (henceforth referred to as *Caprin2*$^{-/-}$) mice where both the alleles

of *Caprin2* are constitutively deleted from the whole body of the mouse. *Caprin2*$^{-/-}$ mice do not exhibit embryonic lethality and are capable of reproducing normally.

2.3 Genotyping

Mouse tail tissue was digested overnight using Direct PCR lysis reagent (Viagen) and Puregene Proteinase K (Qiagen). Proteinase K was heat inactivated at 85°C for 45 minutes. Polymerase Chain Reaction (PCR) was performed with Taq PCR Core Kits (Qiagen). Primers used in PCR were as follows: for *Caprin2* wild type allele, 5'GCCTACCTTTCTGTGCCTCC3' and 5'CCAGGCTACTCTCCCCAAAG3'; for *Caprin2* mutant allele, 5'GCCTACCTTTCTGTGCCTCC3' and 5'TCGTGGTATCGTTATGCGCC3'; for the *Cre* allele, 5'TTCAATTTACTGACCGTACACC3' and 5'CCGACGATGAAGCATGTTTAG3'. PCR products were run on 1% agarose gel containing Ethidium Bromide. Images of the size-separated bands were taken using a GelDoc-It 310 imager (UVP).

2.4 Histology

Whole heads from E14.5 control and mutant mice were collected and fixed overnight in 4% paraformaldehyde (Fisher Scientific) for hematoxylin and eosin (H&E) staining. The samples were then dehydrated with ethanol and embedded in paraffin for microtome sectioning. Sagittal paraffin sections (5 μm) were stained with H&E using a standard protocol (Manthey et al., 2014), examined using light microscopy (Zeiss Axiophot), and imaged with a Nikon digital camera.

2.5 Scanning Electron Microscopy

Scanning electron microscopy (SEM) was performed on 3-month-old control *(Caprin2*$^{+/-}$) and *Caprin2*$^{-/-}$ mutant lenses using an established protocol (Scheiblin et al., 2014). Whole eyes were dissected from control and mutant mice after euthanasia and fixed with a solution containing 0.08 M sodium cacodylate pH 7.4, 1.25% glutaraldehyde, and 1% paraformaldehyde (Electron Microscopy Sciences) for 3hr. Lenses were then dissected from the eye and put in fresh fixative for 48hr. The lenses were washed and the first few layers of the fiber cells were peeled from the lens to reveal either cortical or nuclear fiber cells. The lenses were then transferred to an alcohol dehydration series and hexamethyldisilazane (HMDS, Sigma) dilution series (diluted in ethanol). Lenses were then coated with gold/palladium particles using the Leica EM ACE600 sputter coater for 2.5 min and imaged with the Hitachi S-4700 Field Emission Scanning Electron Microscope. Analysis was performed on three biological replicates for both mutant and control mice.

2.6 Reverse Transcriptase (RT)-quantitative (q) PCR Analysis

Caprin2$^{+/-}$ and *Caprin2*$^{-/-}$ E14.5 mice were euthanized, eyes were excised, and lenses were dissected in 1X RNA-free DPBS (Thermo Scientific). Lenses were then flash frozen at -80°C and stored for later use. Total RNA was extracted using the RNAeasy Mini Kit (Qiagen). RNA concentration was determined using NanoDrop One spectrophotometer (Thermo Scientific). Total RNA was then reverse transcribed into cDNA using the iScript cDNA synthesis kit (Bio-Rad).

qPCR was performed on cDNA samples in technical and biological triplicate using the SYBR Green PCR Master Mix (Invitrogen Life Technology) with 250ng of cDNA included per reaction. Primers used were the aforementioned *Caprin2* exon 5

primers, *Caprin1* and *Gapdh* as a housekeeping gene. Caprin2 primers used were: 5'AGAAAAAGGCCCAGAGAAGG3' and 5'AGGGCAGGTCAGTTTTGAGA3'. Caprin1 primers used were: 5'ACGTCGGGAACAGCTTATGA3' and 5'TGTCACGCTCAGGATCTACG3'. Gapdh primers were: 5'CCGCATCTTCTTGTGCAGT3' and 5'GAATTTGCCGTGAGTGGAGT3'. Each 96-well plate was analyzed on the QuantStudio 6 system (Thermo Fisher). Significance and fold changes were found by ΔΔct and two-level nested variance analysis designed by John McDonald, PhD (Audette 2016).

2.7 Western Blotting

Lenses were enucleated from *Caprin2*$^{+/-}$ and *Caprin2*$^{-/-}$ mice and either flash frozen immediately at -80°C or lysed in lysis buffer (50 mM Tris HCl pH 8.0, 150 mM NaCl, 0.1% sodium dodecyl sulfate (SDS), 1% NP-40 (Tergitol, Sigma-Aldrich), and 0.8% sodium deoxycholate) on ice. Lysed samples were then spun at 14,000g at 4°C for 30 min. The supernatant was collected and protein content was estimated using NanoDrop. 100µg of protein was denatured using 4x Laemmli buffer and loaded and run on a 7% SDS-polyacrylamide gel electrophoresis at 90V for 90 min. Protein was then transferred (at 100V for 1 hour at 4°C) onto a polyvinylidene fluoride membrane (Fisher Scientific) that had been previously soaked in 100% methanol for 5 minutes. The membrane was blocked with 5% in TBST (Tris buffered saline with 1% Tween 20) for 1 hour and incubated overnight at 4°C with rabbit antibodies against Caprin1 and Caprin2 (diluted 1:200 in 5% milk in TBST) (Proteintech Group; Catalog number 15112-1-AP and 20766-1-AP). The blot was then washed with TBST 3 times for 15 minutes each time and incubated for an hour at room temperature with anti-rabbit IgG secondary antibody conjugated to horse radish peroxidase (Cell Signaling).

Three more 15-minute washes were performed with TBST before incubation of the blot with chemiluminescence substrate (GE Healthcare Life Sciences) and being imaged with AlphaImager HP MultiImage II (ProteinSimple).

2.8 Immunofluorescence

E14.5 mouse embryonic head tissue was excised and embedded in tissue freezing media OCT (Tissue Tek) and frozen sections were made at 16µm thickness as described in Lachke et al. 2011. Sections were fixed with 4% PFA in 1x PBS (Phosphate Buffered Saline) for 15 minutes and then washed in 1x PBS with two 10 minute washes. Sections were blocked for 1 hour in 5% goat serum, 1% chicken serum, 0.1% Triton in PBS. Slides were then incubated overnight at 4°C with Caprin1 rabbit primary antibody (1:50 dilution in blocking buffer) (Proteintech Group, Catalog number 15112-1-AP). After this, the slides were washed three times for 15 minutes each in 1x PBS and incubated for 1 hour in a solution of chicken anti-rabbit IgG conjugated to Alexa Fluor 594 secondary antibody (Thermo Fisher Scientific) at 1:200 dilution in blocking buffer and 1:500 dilution of DAPI (4′,6-diamidine-2-phenylidole-dihydrochloride; Life Technologies). Slides were washed three more times with 1x PBS, mounted, and stored at 4°C. Images were taken using Zeiss LSM 780 confocal configured with Argon/Krypton laser (488 nm and 561 nm excitation) and Helium Neon laser (633 nm excitation) (Carl Zeiss Inc.).

Chapter 3

RESULTS

3.1 Generation of *Caprin2* Germline Deletion Mouse Mutants

Caprin2$^{-/-}$ germline knockout mouse mutants were generated through deletion of the fifth exon, that is expected to lead to the nonsense-mediated decay of the resulting transcript that carries a premature stop codon. This was achieved by crossing mice carrying exon 5 flanked by two *loxP* sites with mice carrying Cre recombinase expressed under the control of a human cytomegalovirus (CMV) minimal promoter. The CMV promoter element is expressed in early embryogenesis prior to implantation stage and therefore is expected to cause Cre-mediated deletion of *loxP* flanked genomic region in all tissues. In the resulting *Caprin2* mutants, Cre recombinase recognized the *loxP* sites and deleted exon 5, thereby causing exons 4 and 6 to be spliced together (Figure 3.1A). This leads to a premature stop codon that is expected to resulting in nonsense-mediated decay of the *Caprin2* transcript.

It should be noted that even though the mouse in question has no Caprin2 protein from the beginning of development, we did not observe any embryonic lethality.

3.2 Confirmation of *Caprin2* Germline Deletion

Rearrangement and deletion of *Caprin2* was confirmed in the mouse line using both Western blot and qRT-PCR. Protein was extracted from both *Caprin2*$^{+/-}$ and *Caprin2*$^{-/-}$ lenses at P0 and Western blot analysis was performed. Caprin2 protein was undetectable in *Caprin2*$^{-/-}$ lenses while there was a strong signal in heterozygote lenses

(Figure 3.1B). This indicated that the deletion of *Caprin2* in *Caprin2*$^{-/-}$ mice occurred as expected and resulting in the absence of Caprin2 protein in these mice.

Caprin2 mRNA expression levels in the lenses of E14.5 *Caprin2*$^{-/-}$ mice were examined using qRT-PCR to further confirm knockout. It was found that *Caprin2* was highly downregulated in *Caprin2*$^{-/-}$ mouse lenses, with a 238-fold decrease in expression levels compared to control (Figure 3.1C). Mice were phenotypically normal and no embryonic lethality was observed.

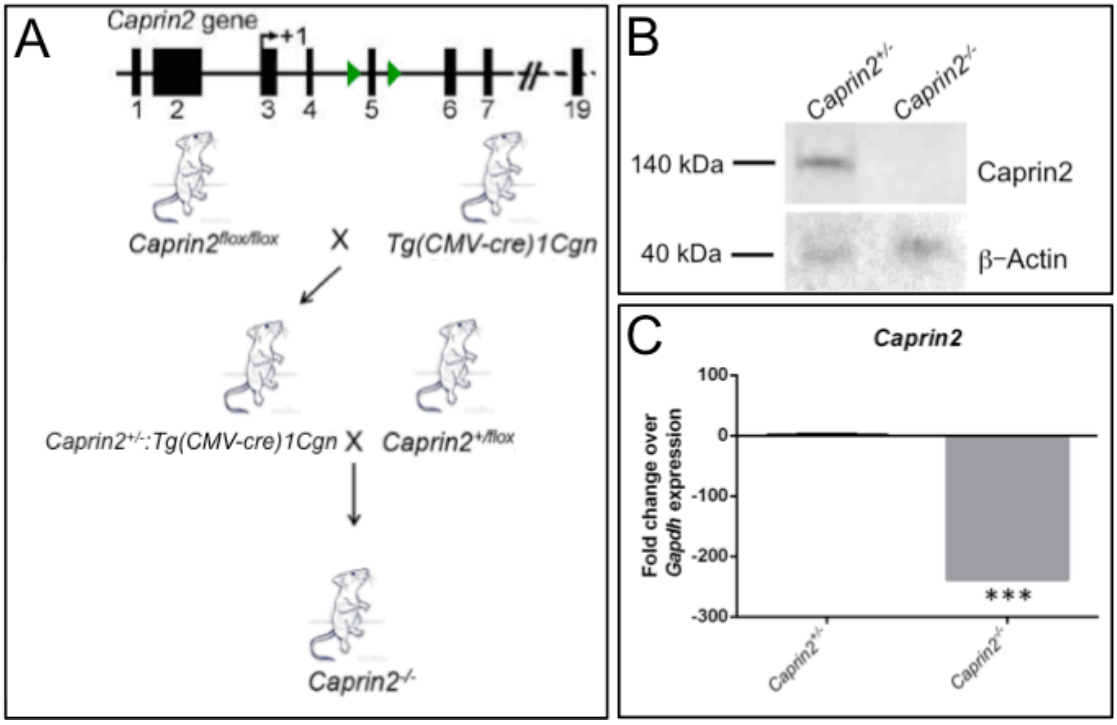

Figure 3.1: Generation of *Caprin2*$^{-/-}$ mice. **A:** Mouse breeding strategy to generate of *Caprin2*$^{-/-}$ mutants. Mice carrying loxP sites (closed arrowheads) flanking the fifth exon of *Caprin2* were crossed with *Tg(CMV-cre)1Cgn* mice expressing Cre recombinase driven by the CMV promoter. This cross provides a progeny that has one *Caprin2* floxed allele and one *Cre* allele, which is further crossed to a mouse with the same genotype (*Caprin2*$^{+/flox}$:*Cre*$^{+/-}$) to generate *Caprin2*$^{-/-}$ mouse. **B:** Confirmation of Caprin2 protein deletion in the mutant mouse lens. Western blotting shows an absence of Caprin2 protein from *Caprin2*$^{-/-}$ lens at P0 (N = 3), while a band is observed in the WT mouse lens. β-actin was used as a loading control. **C:** Comparison of *Caprin2* mRNA expression in control and *Caprin2*$^{-/-}$ lenses. qRT-PCR shows a 238-fold decrease in *Caprin2* expression in *Caprin2*$^{-/-}$ mice. *Gapdh* was used as a housekeeping control.

3.3 Morphology of *Caprin2*$^{-/-}$ Embryonic Mouse Eyes

Whole heads of E14.5 control and mutant mice were processed for histological analysis. H&E staining revealed no discernable difference between *Caprin2*$^{+/-}$ and

Caprin2$^{-/-}$ mouse eyes (Figure 3.4). No ocular defects were observed in *Caprin2*$^{-/-}$ mice.

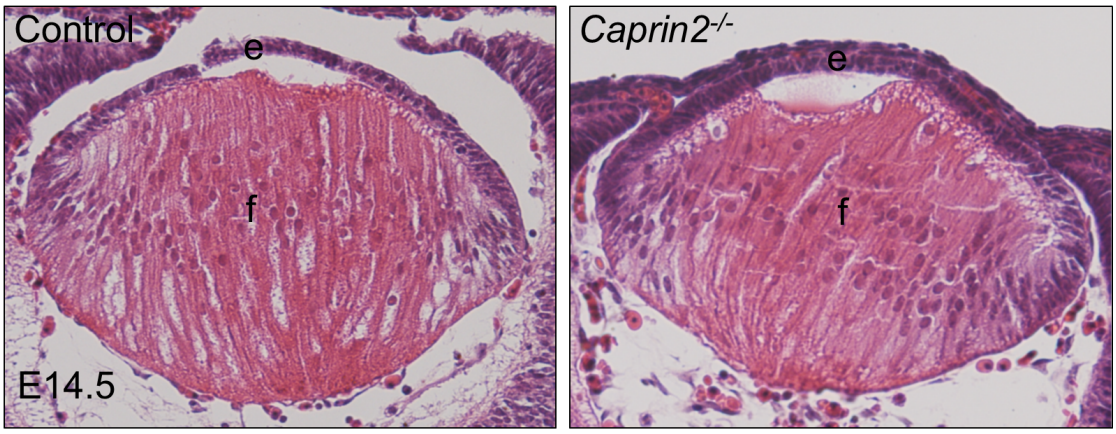

Figure 3.4: Examination of lens morphology in *Caprin2*$^{-/-}$ mutant mice. Histological analysis reveals no defects in E14.5 mouse lenses compared to *Caprin2*$^{+/-}$ controls.

To determine whether lens fiber cell ultrastructure was altered in *Caprin2*$^{-/-}$ mice, scanning electron microscopy was performed on 3-month-old control and mutant lenses. No differences were observed between control and mutant animals in both cortical and nuclear lens fiber cells. Specifically, nuclear compaction defects that were common in *Caprin2*$^{cKO/cKO}$ mice were not observed in *Caprin2*$^{-/-}$ mouse lenses (Figure 3.5).

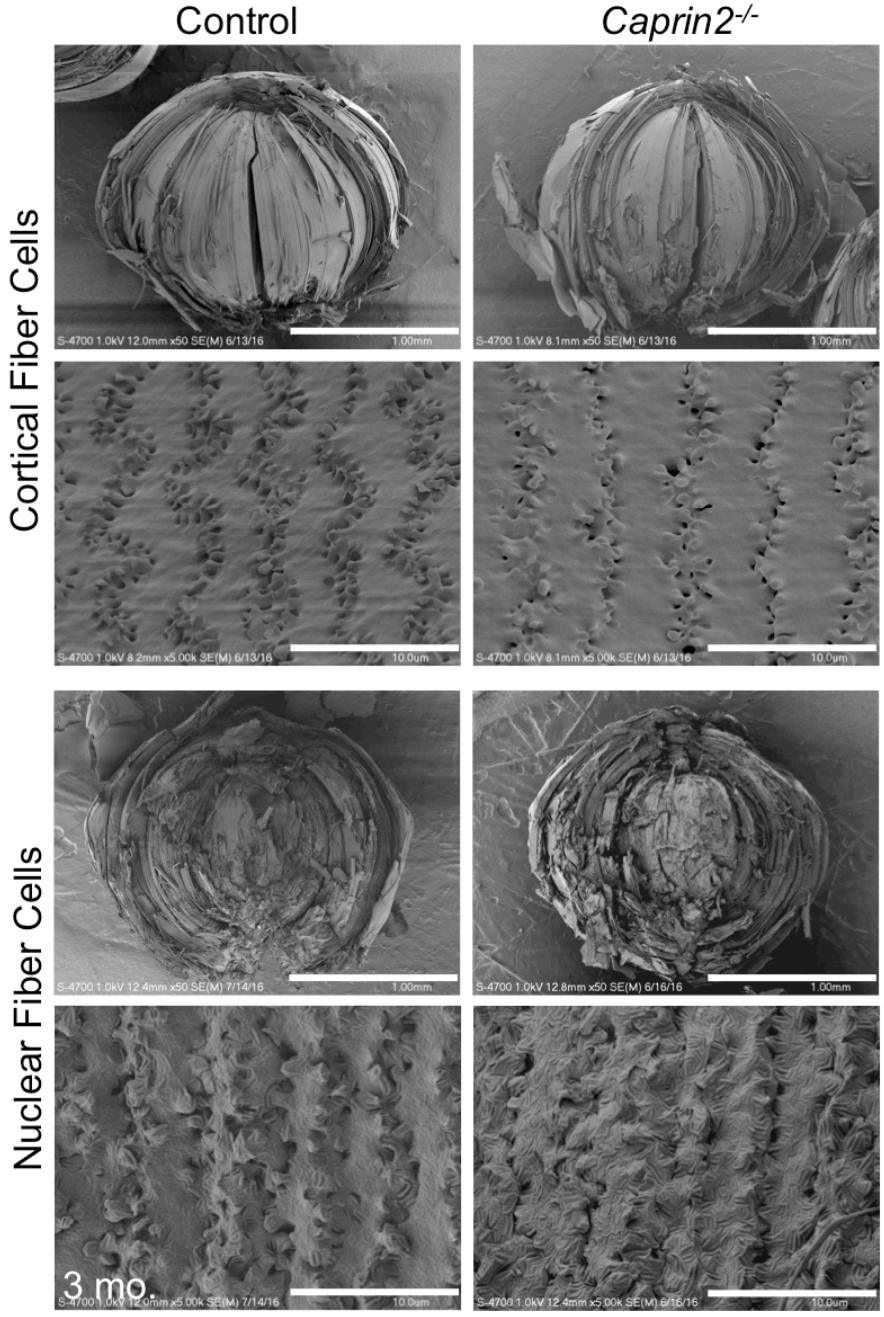

Figure 3.5: *Caprin2*$^{+/-}$ and *Caprin2*$^{-/-}$ lenses have no difference in fiber cell ultrastructure. Scanning electron microscopy of *Caprin2*$^{-/-}$ mutant lenses and age matched controls at age 3 months (N = 3) reveals no significant differences in cortical or nuclear fiber cell ultrastructure.

3.4 Caprin1 Protein and RNA expression in *Caprin2*$^{-/-}$ mice

Caprin2$^{-/-}$ mice exhibit no discernable ocular defects. We hypothesize this could be due to the compensation by upregulation of Caprin1 early in development in *Caprin2*$^{-/-}$ mice. Caprin1 and Caprin2 have similar RNA binding domains. Importantly, Caprin1 is also expressed in the rim of the lens pit at E10.5. However, there was no evidence for the increased expression of its RNA or protein in the *Caprin2*$^{cKO/cKO}$ mice. This could be because the Caprin2 protein was present in the conditional knockout even at a much later stage (E12.5) for the developing eye and therefore may not have led to compensation response resulting from the upregulation Caprin1. In the *Caprin2*$^{-/-}$ mice, Caprin2 is deleted from the start of development. Therefore, it was hypothesized that Caprin1 may exhibit upregulation in *Caprin2*$^{-/-}$ mice in response.

To test this hypothesis, Caprin1 immunostaining was performed on *Caprin2*$^{-/-}$ E11.5 and E14.5 head sections. While there was no significant difference between mutant and controls at E11.5, at stage E14.5, Caprin1 protein was highly expressed in the *Caprin2*$^{-/-}$ lenses compared to the control (Figure 3.6). Further, *Caprin1* mRNA levels were examined in E14.5 *Caprin2*$^{-/-}$ mouse lenses by RT-qPCR analysis. Although it was expected that with increased Caprin1 protein levels in *Caprin2*$^{-/-}$ mouse lenses, there may be a similar increase in *Caprin1* mRNA expression levels, no significant difference was observed (Figure 3.7). These data show that Caprin1 protein is elevated in *Caprin2*$^{-/-}$ mouse lenses offering an explanation to the lack of discernable ocular phenotypes in these animals. However, the mechanism of the Caprin1 protein elevation is not clear at this time, but present findings indicate that it may not involve transcriptional up-regulation of *Caprin1*.

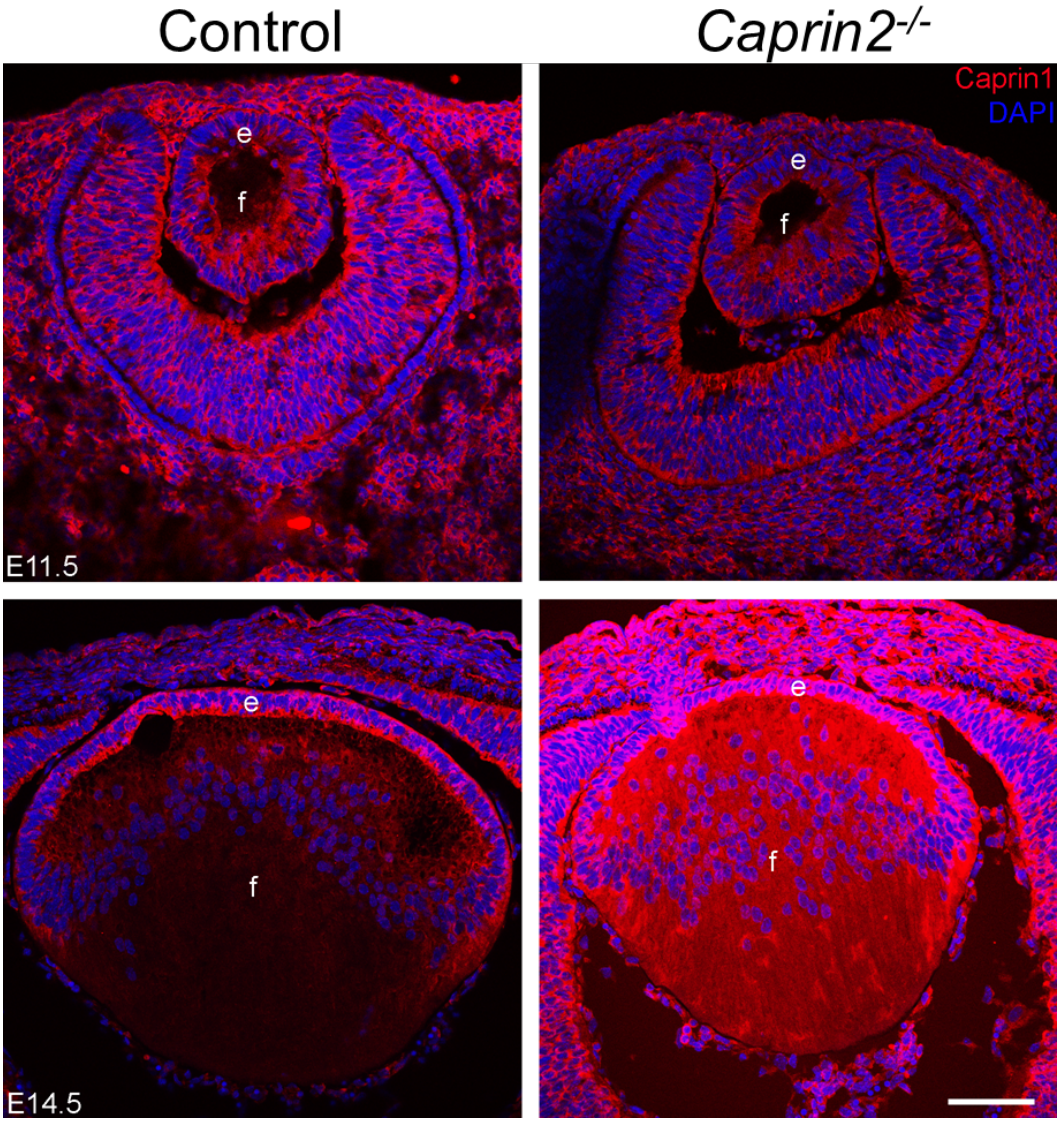

Figure 3.6: Caprin1 expression in *Caprin2*$^{-/-}$ lens. At E11.5, no significant difference was observed in Caprin1 immunostaining between *Caprin2*$^{+/-}$ and *Caprin2*$^{-/-}$ lenses (N = 1). However at E14.5 higher expression of Caprin1 was observed in the fiber cells of the *Caprin2*$^{-/-}$ mice compared to controls (N = 2).

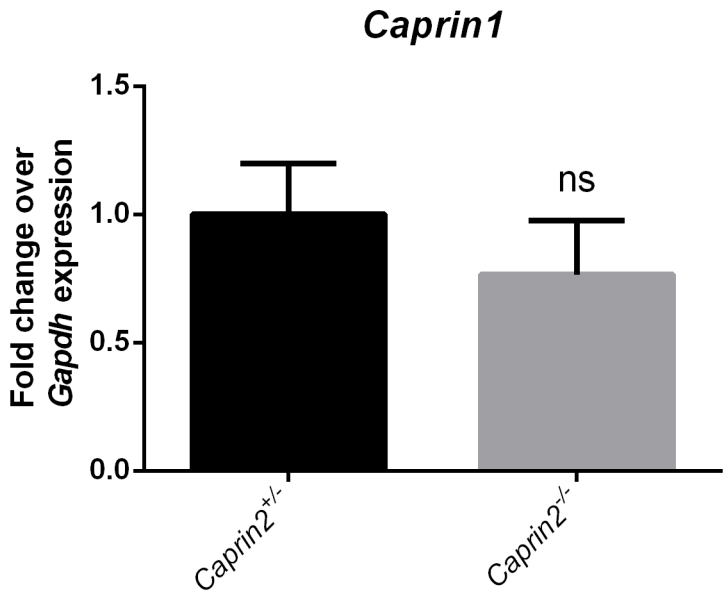

Figure 3.7: *Caprin1* mRNA expression in *Caprin2*$^{-/-}$ lenses. *Caprin1* mRNA is not significantly altered in E14.5 *Caprin2*$^{-/-}$ mouse lenses. *Gapdh* was used as housekeeping control.

Chapter 4

DISCUSSION

Characterization of the targeted conditional knockout of *Caprin2* in the mouse lens raised several new questions about this gene and the mouse model itself. *Caprin2*$^{cKO/cKO}$ mice were generated by breeding *Caprin2*$^{flox/flox}$ mice with mice carrying Cre recombinase under the influence of the *Pax6-P0*-3.9 promoter, which is specifically active in the lens placode (Rowan; 2008, 2010). While the deletion of *Caprin2* in the *Caprin2*$^{cKO/cKO}$ lens was expected at E9.5, residual Caprin2 protein was observed in the E12.5 *Caprin2*$^{cKO/cKO}$ lens. We hypothesized that the presence of residual Caprin2 protein in the *Caprin2*$^{cKO/cKO}$ lenses resulted in the low penetrance of the Peters anomaly-like phenotype observed in these mice. We considered that early removal of Caprin2 may allow us to test this hypothesis. Therefore, we generated *Caprin2* targeted constitutive deletion mouse mutants by crossing *Caprin2*$^{flox/flox}$ mice with mice carrying Cre recombinase under CMV promoter, which is active early in mouse embryogenesis and therefore expected to cause deletion in all tissues. We expected to observe increased ocular phenotype penetrance and severity. Surprisingly, no distinct morphological changes were observed in both histological or scanning electron microscopic analysis between *Caprin2*$^{-/-}$ and control mice.

The absence of phenotypes in *Caprin2*$^{-/-}$ mice could be due to three likely reasons. First, *Caprin2*$^{cKO/cKO}$ mice were maintained on a mixed strain of C57Bl/6 and FVB/N, where *CP49/BFSP2* mutations that have been implicated in lens transparency defects were absent (Simirskii, 2006). *Caprin2*$^{cKO/cKO}$ mice had more characteristics of

the FVB/N background, as the *Caprin2*$^{-/-}$ mice were maintained on a CMV-cre containing C57Bl/6 strain. The genetic background of this mouse strain is known to affect its phenotypic characteristics (Montagutelli, 2000). Hence, *Caprin2*$^{-/-}$ mice should be crossed into FVB/N background to investigate this possibility.

Second, to generate the *Caprin2* null mutants, two different transgenic mice carrying Cre recombinase were used. The *Pax6-P0* promoter was used for generation of *Caprin2*$^{cKO/cKO}$ mice drives the expression of *Pax6* whose mutations have been linked to Peters anomaly (Bhandari, 2011). While immunostaining analysis on *Caprin2*$^{cKO/cKO}$ mice did not reveal any significant difference in Pax6 expression between *Pax6GFPCre:Caprin2*$^{+/cKO}$ and *Caprin2*$^{cKO/cKO}$, expression of other genes linked to Peters anomaly could be significantly altered in these animals. An in depth analysis of Pax6 expression must be performed on *Caprin2*$^{cKO/cKO}$ and *Caprin2*$^{-/-}$ mice.

Third, the loss of Caprin2 in both *Caprin2*$^{cKO/cKO}$ and *Caprin2*$^{-/-}$ could be compensated by a paralog of Caprin2, namely Caprin1, resulting in the low penetrance of phenotype in these mice. Caprin1 is an RNA granule protein, containing RGG boxes and basic helix domains similar to Caprin2. In *Caprin2*$^{cKO/cKO}$ mice, Caprin2 protein is persistent until E12.5 and therefore may not induce a Caprin1 up-regulation response. Comparatively, *Caprin2*$^{-/-}$ mice lack expression of Caprin2 protein altogether and may result in Caprin1 protein upregulation.

Therefore, we examined the expression of Caprin1 mRNA and protein in *Caprin2*$^{-/-}$ lenses. Our analysis revealed that while the levels of *Caprin1* mRNA is not significantly altered in the *Caprin2*$^{-/-}$ lenses, Caprin1 protein was significantly upregulated in the *Caprin2*$^{-/-}$ lenses at E14.5. This suggests that the upregulation of Caprin1 may occur due to post-transcriptional control. Also, these analyses indicated

that surprisingly Caprin1 protein is not upregulated in the E11.5 mouse lenses. Lack of Caprin1 protein upregulation in E11.5 lenses could be due to a lag in Caprin1 compensation because Caprin2 expression begins in the normal lens at E10.5.

This thesis work has laid the groundwork for determining the role of the RNA binding protein Caprin2 in mammalian lens development. Lack of overt phenotype in *Caprin2*$^{-/-}$ mouse has suggested the existence of a redundant protein that acts to compensate for Caprin2 protein function. We have examined a likely candidate, Caprin1, which was shown to be upregulated at E14.5 in *Caprin2*$^{-/-}$ mouse lenses. In addition, lack of significant differences in *Caprin1* mRNA expression provides preliminary evidence for a post-transcriptional mechanism of Caprin1 upregulation. Further work remains to be done to elucidate the connection and larger developmental function of both Caprin1 and Caprin2, a first step toward which may be the generation of *Caprin1* and *Caprin2* double knockout mouse mutants and characterization of their ocular tissues.

Chapter 5

FUTURE DIRECTIONS

This work serves to further characterize the effect of targeted germline knockout of *Caprin2*. While defects in lens fiber cell ultrastructure and lens morphology were not observed in this work, it is still possible that exploration of later time points than 3-months will reveal age-related lens defects. Therefore, to examine lens fiber cell ultrastructure scanning electron microscopy must be performed on *Caprin2*$^{-/-}$ lenses at 6-month and beyond. To test if mouse genetic background difference in *Caprin2*$^{cKO/cKO}$ and *Caprin2*$^{-/-}$ mice is the reason for difference in phenotypes of these mice, *Caprin2*$^{-/-}$ mice should be crossed back to a FVB/N line.

Caprin1 protein has been shown to be upregulated in E14.5 *Caprin2*$^{-/-}$ mouse lenses. Though this preliminary data is promising, the exact relationship between Caprin1 and Caprin2 has yet to be elucidated. Examinations of Caprin1 protein at more embryonic and postnatal time points in *Caprin2*$^{-/-}$ lenses must be performed in order to determine temporally how Caprin1 expression is affected.

To determine if Caprin1 compensates for Caprin2 a preliminary experiment is siRNA knockdown of both Caprin1 and Caprin2 in a lens epithelial cell line. If Caprin1 is indeed compensating for Caprin2, knockdown of both will most likely result in misregulation of key lens genes, possibly including those involved with Peters anomaly. If such misregulation occurs, it would be important to consider a double knockout of *Caprin1* and *Caprin2* in mouse. Characterization of any

phenotypes that result would further understanding of the function of these genes in the development of the lens and eye.

Evidence must also be gathered to determine whether it is specifically Caprin1 that is acting to compensate for the absence of Caprin2 protein in *Caprin2*$^{-/-}$ mice. If it were found that Caprin2 does not bind *Caprin1* mRNA directly, discovery of other possible binding partners for Caprin2 would be required. This is a more long-term goal, however, as the binding partners of Caprin2 have yet to be found.

REFERENCES

Graw, Jochen. "The genetic and molecular basis of congenital eye defects." *Nature Reviews Genetics* 4.11 (2003): 876-888.

Duncan, Melinda K. "A New Focus on RNA in the Lens." *Science* 331.6024 (2011): 1523-1524.

Donaldson, Paul, Joerg Kistler, and Richard T. Mathias. "Molecular solutions to mammalian lens transparency." *Physiology* 16.3 (2001): 118-123.

Cvekl, Aleš, and Ruth Ashery-Padan. "The cellular and molecular mechanisms of vertebrate lens development." *Development* 141.23 (2014): 4432-4447.

Kuszak, J. R., and H. G. Brown. "Embryology and anatomy of the lens."*Principles and practice of ophthalmology. Philadelphia: WB Saunders* (1994): 82-96.

Lang, Richard A., et al. "p120-catenin-dependent junctional recruitment of Shroom3 is required for apical constriction during lens pit morphogenesis." *Development* 141.16 (2014): 3177-3187.

Bassnett, Steven. "On the mechanism of organelle degradation in the vertebrate lens." *Experimental eye research* 88.2 (2009): 133-139.

Shiels, Alan, and J. Fielding Hejtmancik. "Mutations and mechanisms in congenital and age-related cataracts." *Experimental Eye Research* (2016).

Lachke, Salil A., et al. "iSyTE: integrated Systems Tool for Eye gene discovery." *Investigative ophthalmology & visual science* 53.3 (2012): 1617-1627.

Anand, Deepti, and Salil A. Lachke. "Systems biology of lens development: A paradigm for disease gene discovery in the eye." *Experimental eye research* (2016).

Agrawal, S. A., Anand, D., Siddam, A. D., Kakrana, A., Dash, S., Scheiblin, D. A., ... & Motohashi, H. (2015). Compound mouse mutants of bZIP transcription factors Mafg and Mafk reveal a regulatory network of non-crystallin genes associated with cataract. Human genetics, 134(7), 717-735.

Lorén, Christina E., et al. "FGF signals induce Caprin2 expression in the vertebrate lens." *Differentiation* 77.4 (2009): 386-394.

Dash, S., Dang, C. A., Beebe, D. C., & Lachke, S. A. (2015). Deficiency of the RNA binding protein caprin2 causes lens defects and features of peters anomaly. Developmental Dynamics, 244(10), 1313-1327.

Kasaikina, M. V., Fomenko, D. E., Labunskyy, V. M., Lachke, S. A., Qiu, W., Moncaster, J. A., ... & Schweizer, U. (2011). Roles of the 15-kDa selenoprotein (Sep15) in redox homeostasis and cataract development revealed by the analysis of Sep 15 knockout mice. Journal of Biological Chemistry, 286(38), 33203-33212.

Lachke, S. A., Alkuraya, F. S., Kneeland, S. C., Ohn, T., Aboukhalil, A., Howell, G. R., ... & Nair, K. S. (2011). Mutations in the RNA granule component TDRD7 cause cataract and glaucoma.Science, 331(6024), 1571-1576.

Lachke, S. A., Higgins, A. W., Inagaki, M., Saadi, I., Xi, Q., Long, M., ... & Robinson, M. L. (2012). The cell adhesion gene PVRL3 is associated with congenital ocular defects. Human genetics, 131(2), 235-250.

Al-Ghoul, Kristin J., et al. "Structural evidence of human nuclear fiber compaction as a function of ageing and cataractogenesis." *Experimental eye research* 72.3 (2001): 199-214.

Bhandari, Ramanath, et al. "Peters anomaly: review of the literature." *Cornea* 30.8 (2011): 939-944.

Weh, Eric, et al. "Whole exome sequence analysis of Peters anomaly." *Human genetics* 133.12 (2014): 1497-1511.

Sampaolesi, Roberto, Juan Roberto Sampaolesi, and Jorge Zárate. "Ocular Embryology with Special Reference to Chamber Angle Development." *The Glaucomas: Volume I-Pediatric Glaucomas* (2009): 61-69.

Manthey AL, Lachke SA,FitzGerald PG, Mason RW,Scheiblin DA, McDonald JH, Duncan MK. 2014a.Loss of Sip1 leads to migration defects and retention of ectodermal markers during lens development. *Mech Dev***131**:86–110.

Scheiblin DA, Gao J, Caplan JL, Simirskii VN, Czymmek KJ, Mathias RT, Duncan MK. 2014. Beta-1 integrin is important for the structural maintenance and homeostasis of differentiating fiber cells.*Int J Biochem Cell Biol***50**:132–145.

Audette, Dylan S., et al. "Prox1 and fibroblast growth factor receptors form a novel regulatory loop controlling lens fiber differentiation and gene expression." *Development* 143.2 (2016): 318-328.

Rowan, Sheldon, et al. "Notch signaling regulates growth and differentiation in the mammalian lens."*Developmental biology* 321.1 (2008): 111-122.

Rowan, Sheldon, et al. "Precise temporal control of the eye regulatory gene Pax6 via enhancer-binding site affinity." *Genes & development* 24.10 (2010): 980-985.

Simirskii, Vladimir N., et al. "Inbred FVB/N mice are mutant at the cp49/Bfsp2 locus and lack beaded filament proteins in the lens." *Investigative ophthalmology & visual science* 47.11 (2006): 4931-4934.

Montagutelli, Xavier. "Effect of the genetic background on the phenotype of mouse mutations." *Journal of the American Society of Nephrology* 11.suppl 2 (2000): S101-S105.